

Improvement of resistive switching in Cu/ZnO/Pt sandwiches by weakening the randomness of the formation/rupture of Cu filaments

This content has been downloaded from IOPscience. Please scroll down to see the full text.

2011 Nanotechnology 22 275204

(<http://iopscience.iop.org/0957-4484/22/27/275204>)

View [the table of contents for this issue](#), or go to the [journal homepage](#) for more

Download details:

IP Address: 210.72.19.250

This content was downloaded on 01/11/2015 at 06:43

Please note that [terms and conditions apply](#).

Improvement of resistive switching in Cu/ZnO/Pt sandwiches by weakening the randomness of the formation/rupture of Cu filaments

Fei Zhuge^{1,2,3}, Shanshan Peng^{1,2}, Congli He^{1,2}, Xiaojian Zhu^{1,2},
Xinxin Chen^{1,2}, Yiwei Liu^{1,2} and Run-Wei Li^{1,2,4}

¹ Key Laboratory of Magnetic Materials and Devices, Ningbo Institute of Material Technology and Engineering, Chinese Academy of Sciences, Ningbo 315201, People's Republic of China

² Zhejiang Province Key Laboratory of Magnetic Materials and Application Technology, Ningbo Institute of Material Technology and Engineering, Chinese Academy of Sciences, Ningbo 315201, People's Republic of China

³ State Key Laboratory of Silicon Materials, Zhejiang University, Hangzhou 310027, People's Republic of China

E-mail: runweili@nimte.ac.cn

Received 14 April 2011, in final form 10 May 2011

Published 25 May 2011

Online at stacks.iop.org/Nano/22/275204

Abstract

We report an improvement in minimizing the dispersion of resistive switching (RS) parameters such as ON/OFF state resistances and switching voltages of Cu/ZnO/Pt structures in which ZnO films have been deposited at elevated temperature with N doping. This deposition process can enlarge the ZnO grain size and lessen grain boundaries while maintaining a high initial resistance since ZnO naturally shows n-type conductivity and N is a p-type dopant but with a low solubility. Cu filaments with a diameter of 15 nm are found to form at the ZnO grain boundaries. Therefore, fewer grain boundaries could depress the randomness of the formation/rupture of Cu filaments and result in more stable RS performances. Such memory devices show a fast programming speed of 10 ns.

(Some figures in this article are in colour only in the electronic version)

1. Introduction

Resistive random access memory (RRAM) based on the resistive switching (RS) effect has attracted much attention due to its potential for the replacement of flash memory in next generation nonvolatile memory applications [1, 2]. The RS effect was observed from various materials, such as transition metal oxides (TMOs) [3–13], perovskite oxides [14–22], chalcogenide materials [23], carbon-based materials [24–27], and amorphous silicon [28]. Among these, binary TMO-based RRAM has been widely investigated due to the simple compositions of the storage media, in which case the requirements for deposition techniques, temperatures, and substrates are minimized [5]. Among a large variety of binary

TMOs explored for RRAM applications, such as NiO [9, 10], TiO₂ [11], ZnO [5, 8], ZrO₂ [3, 4], and Cu_xO [6, 12], ZnO-based film is one of the most promising semiconductor materials. ZnO-based RRAM devices have been reported to show an ultrafast programming speed of 5 ns, an ultrahigh ON/OFF ratio of 10⁷, a long retention time of more than 10⁷ s, and high reliability at elevated temperatures [5]. However, several problems need to be elucidated before taking into consideration device applications. One of the issues is about minimizing the dispersion of memory switching parameters such as the resistance values of low and high resistance states (LRS and HRS, or ON and OFF) and the required switching voltages from the HRS to the LRS (SET voltages, V_{SET}) and vice versa (RESET voltages, V_{RESET}). In fact, as the device is getting stressed from memory switching cycling,

⁴ Author to whom any correspondence should be addressed.

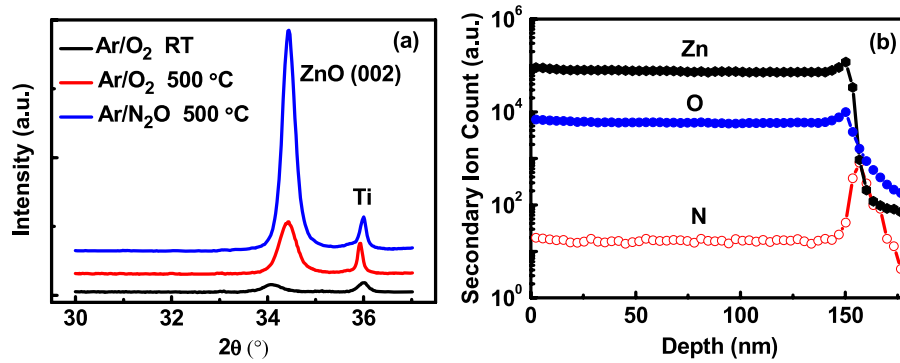


Figure 1. (a) XRD patterns of ZnO films deposited on Pt/Ti/SiO₂/Si substrates at RT, 500 °C in Ar/O₂ ambient, and 500 °C in Ar/N₂O ambient. (b) SIMS depth profiles of ZnO films obtained at 500 °C in Ar/N₂O ambient.

one could observe broad dispersions of these parameters. It would cause severe problems in controlling and reading the memory switching states as a result [29]. For example, large fluctuations in V_{SET} and V_{RESET} may cause a failure in writing and erasing operations, respectively.

In this paper we report an effective method to minimize the dispersions of switching parameters, such as ON/OFF state resistances and SET/RESET voltages, in Cu/ZnO/Pt memory cells in which ZnO films are prepared at 500 °C with N doping. Compared to the samples deposited at room temperature (RT), N-doped ZnO films deposited at 500 °C are composed of coarser grains and fewer grain boundaries while maintain a high initial resistance. The nanoscale Cu filaments are found to form at the ZnO grain boundaries. Fewer grain boundaries could reduce the randomness of the formation/rupture of Cu filaments leading to more stable RS. The devices with N-doped ZnO have a fast switching speed of 10 ns.

2. Experimental details

N-doped ZnO thin films of thickness 150 nm were deposited on Pt/Ti/SiO₂/Si substrates at 500 °C by rf magnetron sputtering in Ar/N₂O ambient (1 Pa, 20% N₂O) using a ceramic ZnO target [30, 31]. The base pressure of the sputtering chamber was less than 2×10^{-4} Pa. Intrinsic ZnO films of thickness 150 nm were also deposited at RT and 500 °C in Ar/O₂ ambient (1 Pa, 20% O₂). In order to measure the electrical properties of the ZnO films, Cu top electrodes of diameter 100 μ m were deposited at RT by electron-beam evaporation with an *in situ* metal shadow mask. The crystal structure and microstructure were examined by x-ray diffraction (XRD), field emission scanning electron microscopy (FESEM), and high resolution transmission electron microscopy (HRTEM), respectively. Secondary ion mass spectroscopy (SIMS; CAMECA IMS-6f) was used to investigate the depth profile of the main elements in the ZnO films. Atomic force microscopy (AFM) was used to detect the surface morphology and leakage current (conductive-AFM (c-AFM) mode). The I - V characteristics of the Cu/ZnO/Pt structures were measured at RT in air using a Keithley 4200 semiconductor parameter analyzer [26, 27]. During the measurement in voltage sweeping mode, the positive bias was defined by the current flowing from the top

to the bottom electrode, and the negative bias was defined by flow in the opposite direction. In the local leakage current measurement by c-AFM, the Pt/Ir coated conductive tip was grounded and directly touched the ZnO films deposited on Cu/Si substrates. Therefore, the same device configuration (Cu/ZnO/Pt) was used for c-AFM and I - V measurements. The resistances in the LRS and HRS of the Cu/ZnO/Pt structures were measured as a function of temperature by a physical properties measurement system (PPMS; Quantum Design). The test of switching speed was performed using an Agilent 81110A pulse/pattern generator and a LeCroy WaveRunner 62Xi digital storage oscilloscope [32].

3. Results and discussion

The XRD patterns of the ZnO thin films deposited on the Pt/Ti/SiO₂/Si substrates are shown in figure 1(a). All the films exhibit a highly (002) textured orientation. The (002) XRD peaks of the samples deposited at 500 °C are much stronger. Furthermore, compared to the intrinsic ZnO deposited at 500 °C, the intensity of the (002) peak for the N-doped ZnO is higher, probably due to N₂O being a stronger oxidizing agent than O₂ [33, 34]. Figure 1(b) exhibits the typical SIMS depth profiles of the main elements in the ZnO films deposited at 500 °C in Ar/N₂O. Although the absolute value of the N concentration cannot be obtained from figure 1(b), it is clear that the films are doped with N, as intended. There appears to be a large N segregation at the substrate/film interface, with the caveat that SIMS measurements are sometimes subject to artifacts at surfaces and interfaces [35, 36].

The intrinsic ZnO film deposited at RT with an initial resistance $>10^7 \Omega$ shows bipolar RS behavior, as shown in figure 2(a). No RS phenomenon is observed for the intrinsic ZnO deposited at 500 °C with a small initial resistance of about 6 Ω (figure 2(b)), which is even lower than that of the LRS in figure 2(a) (about 30 Ω). For polycrystalline intrinsic ZnO films prepared at elevated temperatures, the electron concentration and Hall mobility can reach 10^{19} cm^{-3} and $10 \text{ cm}^2 \text{ V}^{-1} \text{ s}^{-1}$, respectively, resulting in a low resistivity of $\sim 10^{-2} \Omega \text{ cm}$ [37]. It is always difficult to observe RS phenomena in ZnO films with a very low initial resistance [5, 8, 38, 39]. However, the bipolar RS phenomenon

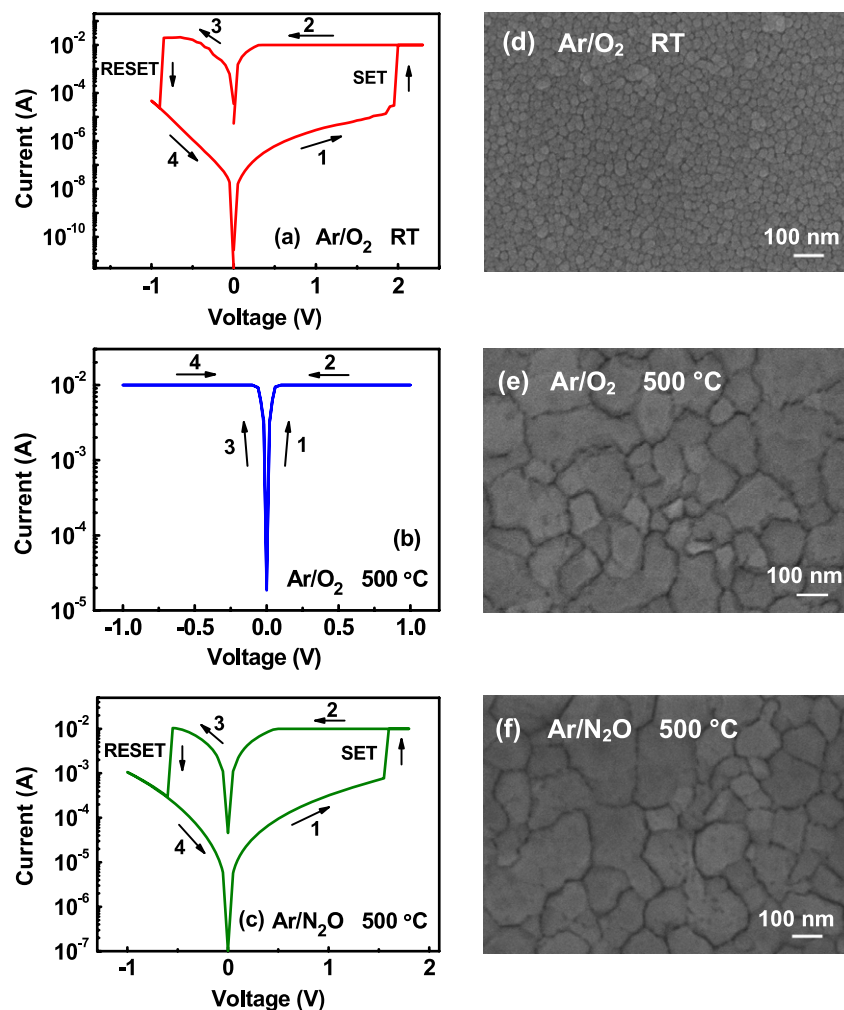


Figure 2. Typical I – V characteristics of (a) the intrinsic ZnO films deposited at RT, (b) the intrinsic ZnO films obtained at 500 °C, and (c) the N-doped ZnO films. FESEM images of (d) the intrinsic ZnO films obtained at RT, (e) the intrinsic ZnO films deposited at 500 °C, and (f) the N-doped ZnO films.

is observed for the N-doped ZnO film deposited at 500 °C, which exhibits an initial resistance of $>10^4 \Omega$, as shown in figure 2(c). As we know, N is an acceptor but with low solubility in ZnO. Although it is difficult to achieve high-hole-concentration p-type ZnO films by N doping, the electrons induced by the native point defects such as oxygen vacancies and zinc interstitials will be partially compensated by the incorporation of N, resulting in highly resistive ZnO films even if deposited at elevated temperatures [30, 35]. Therefore, the N-doped ZnO films deposited at 500 °C maintain a high initial resistance and make the occurrence of the RS possible. Considering that copper was used as the top electrode, CuO_x may form at the Cu/ZnO interface during the deposition process. To eliminate the possibility that the observed RS results from the combination of both ZnO and CuO_x layers rather than pure ZnO, cross section TEM measurements were performed. Figures 3(a) and (b) show a low-magnification TEM image and HRTEM image for the Cu/intrinsic ZnO (RT)/Pt cell, while figures 3(c) and (d) show the corresponding TEM images for the Cu/N-doped ZnO/Pt cell. From figure 3, we can see that Cu and ZnO layers have a clear interface and

no CuO_x layer can be observed. Therefore, it is confirmed that the observed RS comes from ZnO.

Figures 4(a) and (b) show the endurance characteristics of the intrinsic ZnO film deposited at RT and N-doped film, respectively. The resistance values were read out at 0.1 V in each sweep. It is clear that the N-doped film exhibits more stable resistive values in both the HRS and LRS than the intrinsic one, especially for the HRS. Figures 4(c) and (d) illustrate the evolution of V_{SET} and V_{RESET} of the intrinsic and N-doped ZnO within 100 switching cycles, respectively. The dispersions of V_{SET} and V_{RESET} for the N-doped film are visibly reduced in comparison with the intrinsic one, especially for V_{SET} . The average values of V_{SET} and V_{RESET} of the N-doped film are about 1.47 and -0.45 V, respectively, which are lower than the values of the intrinsic one (1.96 and -0.78 V), respectively. Therefore, the N-doped ZnO film deposited at 500 °C shows significant advantages over the intrinsic ZnO film prepared at RT for memory applications in terms of stable switching phenomena and low switching voltages.

To understand the switching mechanism of the ZnO films, the resistance in the LRS (R_{ON}) of the N-doped ZnO film was

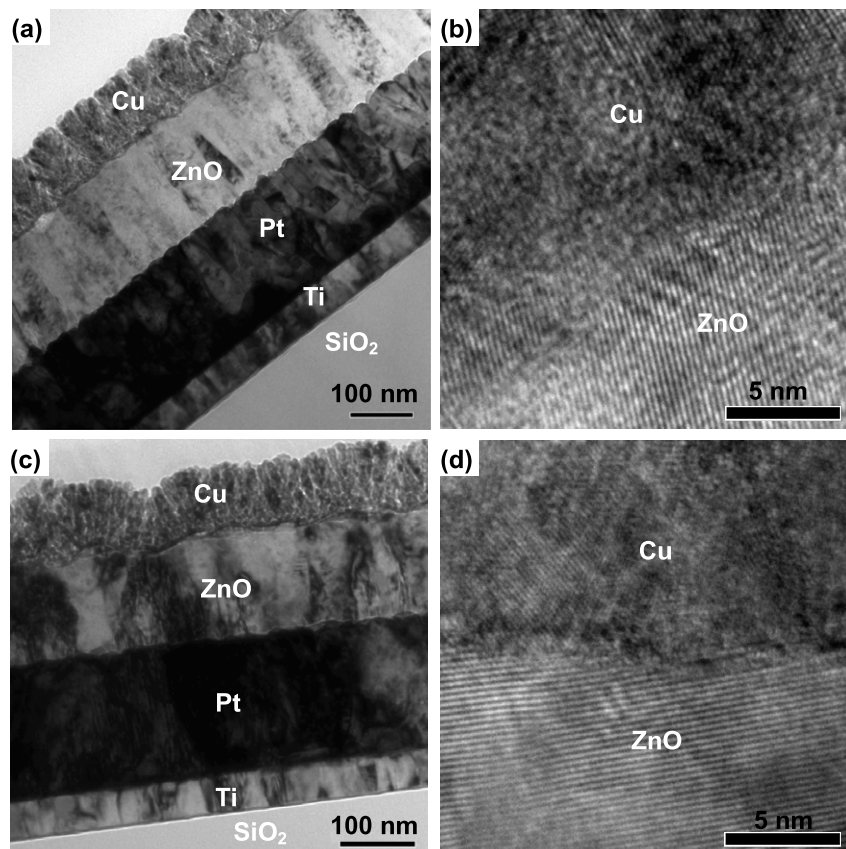


Figure 3. (a) A low-magnification cross section TEM image, and (b) HRTEM image for the Cu/intrinsic ZnO (RT)/Pt cell. (c) A low-magnification cross section TEM image, and (d) HRTEM image for the Cu/N-doped ZnO/Pt cell.

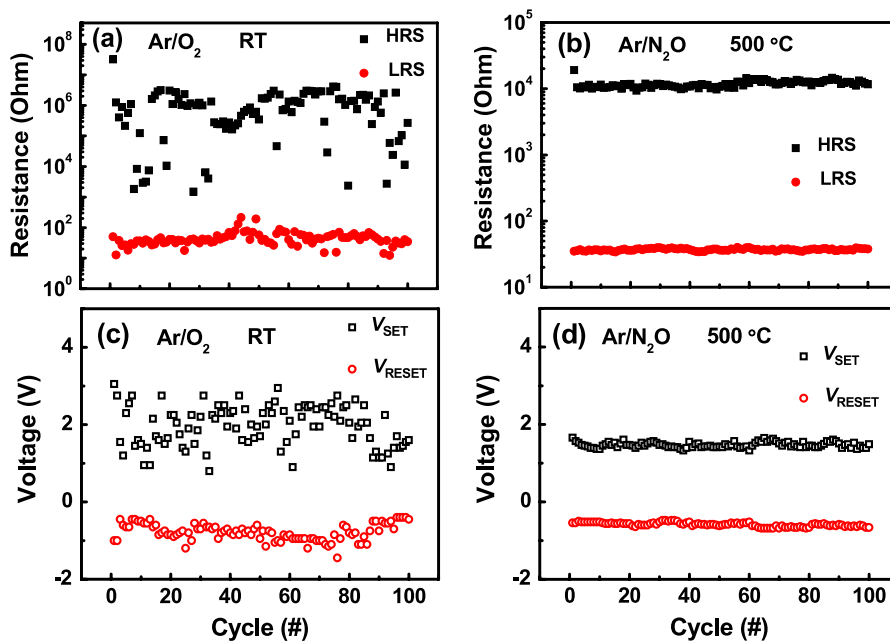


Figure 4. (a) Endurance performance of the intrinsic ZnO deposited at RT. (b) Endurance performance of the N-doped ZnO. (c) Evolution of V_{SET} and V_{RESET} of the intrinsic ZnO deposited at RT. (d) Evolution of V_{SET} and V_{RESET} of the N-doped ZnO.

measured as a function of temperature. Figure 5 shows the typical metallic behavior of R_{ON} . The metallic conducting behavior in the LRS indicates the formation of conducting

filaments in the ZnO films [27]. On the other hand, the resistance in the HRS of the N-doped ZnO film is found to decrease with increasing temperature, and it exhibits a typical

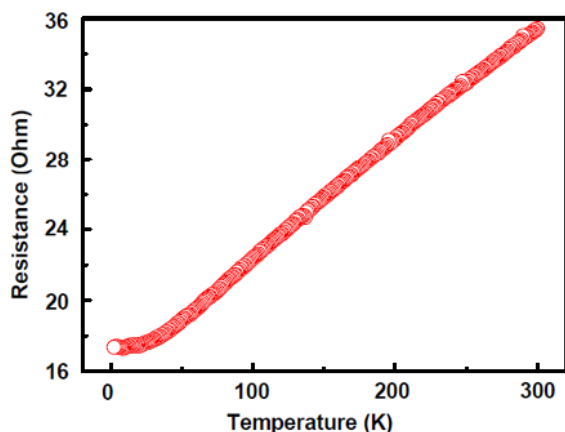


Figure 5. Temperature dependence of the resistance in the LRS of the N-doped ZnO films.

semiconducting behavior. Thus, the observed RS effect in the ZnO films could be attributed to the formation/rupture of conducting filaments. This is consistent with the results reported by other groups [5, 8, 38, 39]. The temperature dependence of metallic resistance can be written as $R(T) = R_0[1 + \alpha(T - T_0)]$, where R_0 is the resistance at temperature T_0 , and α is the temperature coefficient of resistance. By choosing T_0 as 300 K, the α of the filaments is calculated to be $2.26 \times 10^{-3} \text{ K}^{-1}$, which is similar to the value of 2.5×10^{-3} for high-purity Cu nanowires of diameter $\geq 15 \text{ nm}$ [40], indicating that the filaments are composed of Cu in metallic states due to the diffusion of the top electrode under a bias voltage. The discrepancy of α is attributed to inevitable defects in the

Cu filaments, since the presence of defects can reduce α by shortening the mean free path of electrons [40, 41]. It is known that extended defects, such as grain boundaries and dislocations, provide easy diffusion paths for oxygen vacancies or metal ions in metallic oxides [8, 42]. The point defects, such as oxygen vacancies or metal ions, prefer to form and gather around the grain boundaries. The AFM and c-AFM images of the ZnO films deposited at RT at OFF and ON states are shown in figure 6. No obvious leakage current is detected under a read voltage of 1 V for the OFF state. After applying a large voltage of 10 V, several conducting nanobits with a diameter of about 15 nm are observed under a read voltage of 1 V, confirming that a certain number of conducting filaments exist in the ON-state samples. Furthermore, by comparing figures 6(b) and (d), we find that the conducting nanobits locate at the grain boundaries of ZnO, verifying that the Cu filaments form at the grain boundaries. A similar phenomenon (i.e. the nanoscale conducting nanobits locate at the grain boundaries of ZnO) has also been observed by c-AFM for high-temperature N-doped ZnO. Figures 2(d)–(f) show the FESEM images of the intrinsic ZnO film prepared at RT, intrinsic film obtained at 500 °C, and N-doped film deposited at 500 °C, respectively. It is obvious that depositing ZnO films at elevated temperature leads to coarser grains and thus fewer grain boundaries. For the N-doped ZnO films prepared at elevated temperature with fewer grain boundaries, the formation and rupture of Cu filaments will be less random, resulting in more stable RS performances. Furthermore, the strongly preferred (002)-orientation of N-doped ZnO films suggests a highly ordered arrangement of grain boundaries. This is also favorable for the formation of the Cu filaments with less randomness and leads to more stable RS behaviors.

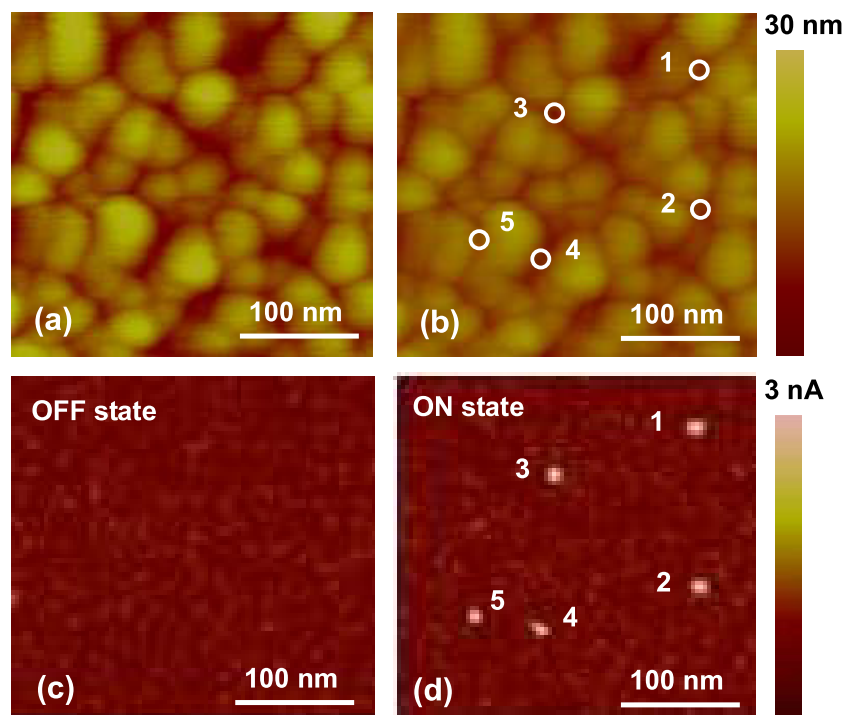


Figure 6. (a) AFM and (c) c-AFM images of the intrinsic ZnO films deposited at RT in the OFF state under a read voltage of 1 V. (b) AFM and (d) c-AFM images of the intrinsic ZnO films deposited at RT in the ON state under a read voltage of 1 V. The same numbers represent the same regions.

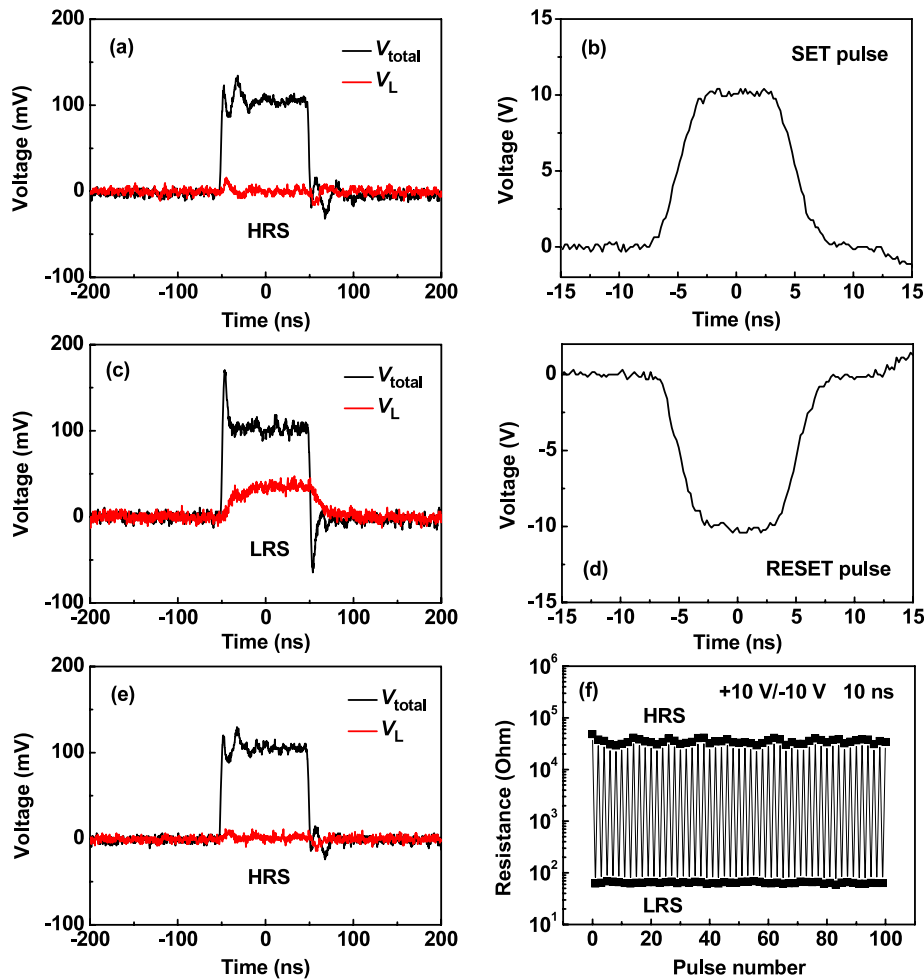


Figure 7. Measures of the switching speed of Cu/N-doped ZnO/Pt memory cells. (a) A reading voltage of 100 mV with 100 ns duration confirms the initial HRS. (b) A SET pulse of 10 V with 10 ns duration was applied to the cell. (c) The subsequent reading signal confirms the final LRS. (d) A RESET pulse of -10 V with 10 ns duration was applied to the cell. (e) The reading signal confirms that the cell is switched back to the HRS. (f) Write/erase cycles of the Cu/N-doped ZnO/Pt device by a 10 V, 10 ns pulse for writing and a -10 V, 10 ns pulse for erasing.

For measurement of the switching speed of the Cu/N-doped ZnO/Pt memory device, the device was put in series to a load resistance R_L (47Ω). The schematic configuration of the measurement system is described in [32]. The change in the resistance state can be detected by measuring the voltage dropped on the load resistance (V_L), which can be written as $V_L = V_{total} R_L / (R_{device} + R_L)$, where R_{device} is the device resistance and V_{total} is the total voltage dropped on R_L and R_{device} . As the device is in the HRS, almost all the V_{total} drops on the device since R_{device} ($\sim 10^4 \Omega$) is much larger than R_L . So, V_L should approach zero, as shown in figure 7(a) (employing a reading voltage pulse of 100 mV with 100 ns duration). While for the memory device in the LRS, V_L is comparable to V_{device} since R_{device} ($\sim 30 \Omega$) and R_L have a close value. Therefore, after applying a 10 V, 10 ns pulse (figure 7(b)), the device is switched to the LRS (figure 7(c)). After applying a -10 V, 10 ns pulse (figure 7(d)), the device is switched back to the HRS (figure 7(e)). Figure 7(f) shows write/erase cycles of the Cu/N-doped ZnO/Pt device by a 10 V, 10 ns pulse for writing and a -10 V, 10 ns pulse for erasing. Our results demonstrate that the memory cell could be

programmed by a 10 V, 10 ns SET pulse and a -10 V, 10 ns RESET pulse, respectively.

4. Summary

In summary, we have shown that the RS properties of Cu/ZnO/Pt memory cells can be improved by doping ZnO with N at elevated temperature. The formation of nanoscale Cu filaments at the grain boundaries of ZnO is confirmed by c-AFM measurements. N-doped ZnO films prepared at elevated temperature have larger grains and fewer grain boundaries while maintaining a high initial resistance. A decrease in the number of grain boundaries is favorable for depressing the randomness of the formation and rupture of Cu filaments, resulting in more stable RS behaviors. The memory cells have a high switching speed of 10 ns.

Acknowledgments

We thank X Gao and Y D Xia for the measurement of switching speed. This work was supported by State Key

Research Program of China (973 Program), National Natural Science Foundation of China, Zhejiang and Ningbo Natural Science Foundations, Chinese Academy of Sciences (CAS), Zhejiang Qianjiang Talent Project, and State Key Lab of Silicon Materials (China).

References

- [1] Waser R and Aono M 2007 *Nat. Mater.* **6** 833
- [2] Strukov D, Snider G, Stewart D and Williams R 2008 *Nature* **453** 80
- [3] Liu M, Abid Z, Wang W, He X L, Liu Q and Guan W H 2009 *Appl. Phys. Lett.* **94** 233106
- [4] Liu Q, Long S B, Wang W, Zuo Q Y, Zhang S, Chen J N and Liu M 2009 *IEEE Electron Device Lett.* **30** 1335
- [5] Yang Y C, Pan F, Liu Q, Liu M and Zeng F 2009 *Nano Lett.* **9** 1636
- [6] Lv H B, Yin M, Song Y L, Fu X F, Tang L, Zhou P, Zhao C H, Tang T A, Chen B A and Lin Y Y 2008 *IEEE Electron Device Lett.* **29** 47
- [7] Shang D S, Shi L, Sun J R, Shen B G, Zhuge F, Li R W and Zhao Y G 2010 *Appl. Phys. Lett.* **96** 072103
- [8] Chang W Y, Lai Y C, Wu T B, Wang S F, Chen F and Tsai M J 2008 *Appl. Phys. Lett.* **92** 022110
- [9] Seo S et al 2004 *Appl. Phys. Lett.* **85** 5655
- [10] Lee M J et al 2007 *Adv. Mater.* **19** 3919
- [11] Kwon D H et al 2010 *Nat. Nanotechnol.* **5** 148
- [12] Fujiwara K, Nemoto T, Rozenberg M J, Nakamura Y and Takagi H 2008 *Japan. J. Appl. Phys.* **47** 6266
- [13] Inoue I H, Yasuda S, Akinaga H and Takagi H 2008 *Phys. Rev. B* **77** 035105
- [14] Liu S Q, Wu N J and Ignatiev A 2000 *Appl. Phys. Lett.* **76** 2749
- [15] Beck A, Bednorz J G, Gerber C, Rossel C and Widmer D 2000 *Appl. Phys. Lett.* **77** 139
- [16] Liao Z L, Wang Z Z, Meng Y, Liu Z Y, Gao P, Gang J L, Zhao H W, Liang X J, Bai X D and Chen D M 2009 *Appl. Phys. Lett.* **94** 253503
- [17] Dong R, Wang Q, Chen L D, Shang D S, Chen T L, Li X M and Zhang W Q 2005 *Appl. Phys. Lett.* **86** 172107
- [18] Xia Y D, Liu Z G, Wang Y, Shi L, Chen L, Yin J and Meng X K 2007 *Appl. Phys. Lett.* **91** 102904
- [19] Sawa A, Fujii T, Kawasaki M and Tokura Y 2006 *Appl. Phys. Lett.* **88** 232112
- [20] Odagawa A, Sato H, Inoue I H, Akoh H, Kawasaki M and Tokura Y 2004 *Phys. Rev. B* **70** 224403
- [21] Li M, Zhuge F, Zhu X J, Yin K B, Wang J Z, Liu Y W, He C L, Chen B and Li R W 2010 *Nanotechnology* **21** 425202
- [22] Yin K B, Li M, Liu Y W, He C L, Zhuge F, Chen B, Lu W, Pan X Q and Li R W 2010 *Appl. Phys. Lett.* **97** 042101
- [23] Ma L P, Liu J and Yang Y 2002 *Appl. Phys. Lett.* **80** 2997
- [24] Sinitskii A and Tour J M 2009 *ACS Nano* **3** 2760
- [25] Standley B, Bao W Z, Zhang H, Bruck J, Lau C N and Bockrath M 2008 *Nano Lett.* **8** 3345
- [26] He C L et al 2009 *Appl. Phys. Lett.* **95** 232101
- [27] Zhuge F, Dai W, He C L, Wang A Y, Liu Y W, Li M, Wu Y H, Cui P and Li R W 2010 *Appl. Phys. Lett.* **96** 163505
- [28] Jo S H and Lu W 2008 *Nano Lett.* **8** 392
- [29] Kim D C et al 2006 *Appl. Phys. Lett.* **88** 232106
- [30] Lu J G, Ye Z Z, Zhuge F, Zeng Y J, Zhao B H and Zhu L P 2004 *Appl. Phys. Lett.* **85** 3134
- [31] Zhuge F, Zhu L P, Ye Z Z, Ma D W, Lu J G, Huang J Y, Wang F Z, Ji Z G and Zhang S B 2005 *Appl. Phys. Lett.* **87** 092103
- [32] Gao X et al 2010 *J. Appl. Phys.* **108** 074506
- [33] Zhuge F, Zhu L P, Ye Z Z, Lu J G, Zhao B H, Huang J Y, Wang L, Zhang Z H and Ji Z G 2005 *Thin Solid Films* **476** 272
- [34] Lau W S, Qian P W, Han T, Sandler N P, Che S T, Ang S E, Tung C H and Sheng T T 2007 *Microelectron. Reliab.* **47** 429
- [35] Ye Z Z, Zhuge F, Lu J G, Zhang Z H, Zhu L P, Zhao B H and Huang J Y 2004 *J. Cryst. Growth* **265** 127
- [36] Zhuge F, Zhu L P, Ye Z Z, Lu J G, He H P and Zhao B H 2007 *Chem. Phys. Lett.* **437** 203
- [37] Bian J M, Li X M, Zhang C Y, Chen L D and Yao Q 2004 *Appl. Phys. Lett.* **84** 3783
- [38] Seo J W, Park J W, Lim K S, Yang J H and Kang S J 2008 *Appl. Phys. Lett.* **93** 223505
- [39] Xu N, Liu L F, Sun X, Liu X Y, Han D D, Wang Y, Han R Q, Kang J F and Yu B 2008 *Appl. Phys. Lett.* **92** 232112
- [40] Bid A, Bora A and Raychaudhuri A 2006 *Phys. Rev. B* **74** 035426
- [41] Mooij J H 1973 *Phys. Status Solidi a* **17** 521
- [42] Sztot K, Speier W, Carius R, Zastrow U and Beyer W 2002 *Phys. Rev. Lett.* **88** 075508